1   Electronic Supplemental Information for:

2   **MoS₂−modified Graphite Felt as High Performance Electrode Material**

3   **for Zinc−polyiodide Redox Flow Battery**

4   Jian Liu,[a] Ting Ma,[a] Meng Zhou,[a] Shuang Liu,[a] Jin Xiao,[b,c] Zhanliang Tao*[a] and Jun Chen [a]

5

6   [a]Key Laboratory of Advanced Energy Materials Chemistry (Ministry of Education), College

7   of Chemistry, Nankai University, Tianjin 300071, China.

8   [b]School of Science, Hunan University of Technology, Zhuzhou 412007, China

9   [c]State Key Laboratory of Superlattices and Microstructures, Institute of Semiconductors

10   Chinese Academy of Sciences, Beijing 100083, China

11

12

13

14

15

16

17

18

19

20

21

22

23

24

25   *To whom correspondence should be addressed.

26   Email: taozhl@nankai.edu.cn

Experimental Section

Pretreating of graphite felts (GF): To avoid impurities and enhance wettability, pristine GF were pretreated by several steps before used. Firstly, GF were rinsed in acetone overnight and then dried in air at 80 ℃. Secondly, a solution of 200 g/L ammonium persulphate $((NH_4)_2S_2O_8)$ in 100 mL/L sulfuric acid was prepared. Thirdly, the GF were rinsed in the acid solution and ultra−sonicated for 15 min and then washed by DI−water and ethanol several times. Finally, GF were thermal treated at 450 ℃ for 30 min.

Synthesis of MoS₂ nanoplates and MoS₂ nanoplates modified GF: All chemicals for this experiment were used directly without further purification. Pure MoS₂ nanoplates were synthesized according to a previous report[1]. In a typical synthesis process, 20 mg ammonium thiomolybdate $((NH_4)_2MoS_4$, Sigama−Aldrich) was dispersed in the mixture (15 mL) of N, N−Dimethylformamide (DMF) and deionized (DI) water with volume ratio of 2:1 mixture. The mixture was ultra−sonicated for 30 min and then transferred into the autoclave, and maintained at 210 ℃ for 12 h. After cooling to room temperature naturally, the black precipitate was collected and washed by DI water and ethanol several times, and finally dried at 80 ℃ for 12h. To introduce MoS₂ nanoplates on the surface of GF, the GF were placed inside the precursor solution with different amount $(NH_4)_2MoS_4$ (15, 20, 25 mg), denoted as 15 mg, 20 mg, 25 mg MoS₂@GF. After cooling to room temperature, the modified GF were rinsed with DI water several times until no obvious MoS₂ particles were observed in the wastewater stream. Then the modified GF electrodes were dried at 80 ℃ for 12h.

Preparation of Zn²⁺−form Nafion membranes: The Zn²⁺−form Nafion membranes (N−115 from Hesen, Shanghai, China, active area of 4 cm²) were pretreated prior to use with the following steps: i) The Nafion membrane was soaked in 3 wt% H_2O_2 aqueous solution at 60 ℃ for 1 hour. Then it was washed with DI water to remove the remaining H_2O_2; ii) The Nafion membrane was soaked in 0.5 M H_2SO_4 at 60 ℃ for 1 hour and washed with DI water; iii) It was

52 soaked in 1 M $ZnCl_2$ aqueous solution (pH was adjusted to 1 by using HCl) at 60 °C for 3 hours

53 to covert from the H^+−form to the Zn^{2+}−form. Then the membrane was rinsed with DI water

54 and stored in DI water.

55 **Characterization:** All transmission electron microscopy (TEM) images and elemental

56 mapping were taken from FEI Tecnai G2 F30S−Twin microscope, 300 kV. The morphology

57 were recorded by scanning electron microscope (JSM−7800F). XRD analysis of different

58 samples was carried out on a X−ray diffractometer (Bruker AXS D8, Cu Kλ, λ = 1.5406 Å, 40

59 kV and 20 mA). X−ray photoelectron spectroscopy (XPS) spectrum was measured on a VG

60 Escalab 250 spectrometer equipped with an Al anode (Al Kα = 1846.6 eV). N_2

61 adsorption/desorption isotherm was conduct to analyze the pore structure. The BET surface

62 area was determined using adsorption data in the relative pressure (P/P_0) range of 0.05−0.25.

63 The presence of I_3^-/I^- in the compartment was determined by ultraviolet−visual spectroscopy

64 using a UV−Vis spectrometer (JASCO V−550).

65 **Electrochemical measurements:** All electrochemical measurements were conducted on a

66 VersaSTAT potentiostat/galvanostat (Princeton Applied Research) using a standard three

67 electrode set−up with a glassy carbon disk working electrode (5 mm diameter), a Ag/AgCl

68 reference electrode, and a Pt counter electrode at room temperature. The working electrode was

69 prepared on a glass carbon (GC) disk as the substrate. Typically, a mixture containing 3.0 mg

70 catalyst, 7.0 mg Vulcan carbon 72, 1.0 mL ethanol and 0.05 mL Nafion solution (0.05 wt%,

71 Hesen) was ultrasonicated for 30 min to obtain a well−dispersed ink. Then 10 μl of the catalyst

72 ink (containing 28.6 μg of catalyst) was loaded onto a glassy carbon electrode (loading ∼ 0.136

73 $mg \cdot cm^{-2}$). The presented current density refers to the geometric surface area of the glass carbon

74 electrode.

75 **Charging/Discharging Tests:** The configuration and photographs of the components of the

76 non-flow cell are shown in Figure S11. Generally, in the positive half−cell, a piece of graphite

77 felt (2.5 mm thickness and active geometric area of 1 cm^2) was used as the electrode and a

78 titanium wire was used as the current collector. As for the negative half−cell, zinc plate with a

79 diameter of 12 mm was tin soldered on a titanium, serving as the electrode and current collector.

80 The cell assembly was finished in the ambient air and then transferred to the argon−filled glove

81 box. Active electrolyte with a volume of 2.5 mL was injected in each half−cell. The charge

82 capacity was fixed to be 60% of the state of charge (SOC) in order to avoid unstable zinc

83 electrolytic deposition/dissolution and improve the cyclic performance. The electrolytes were

84 prepared by dissolving corresponding ZnI_2 (Jindian Chemical Co. Ltd., China, 99%) in an

85 Argon (Ar)−saturated DI water in an Ar−filled glove box.

86 **Theoretical methord:** Quantum chemistry calculations were carried out using the Vienna

87 Ab−initio Simulation Package (VASP). The generalized gradient approximation (GGA) of the

88 Perdew–Burke–Ernzerhof (PBE) exchange correlation function[1] was adopted with the

89 plane−wave cutoff energy set at 400 eV. The criterion of convergence was set that the residual

90 forces are less than 0.02 eV/Å and the change of the total energy was less than 10^{-4} eV. The

91 simulation was conducted assuming a vacuum condition.

92   The E_{ad}^I on the surface of the catalyst can be defined as follows[2]:

93
$$E_{ad}^I = E_{interface} + 1/2\, E_{I_2} - E_{I/interface}$$

94 where $E_{interface}$, E_{I_2} and $E_{I/interface}$ represent the energies of the liquid/electrode interface, I_2 in the

95 gas phase and the liquid/electrode interface with the adsorbed I atoms, respectively.
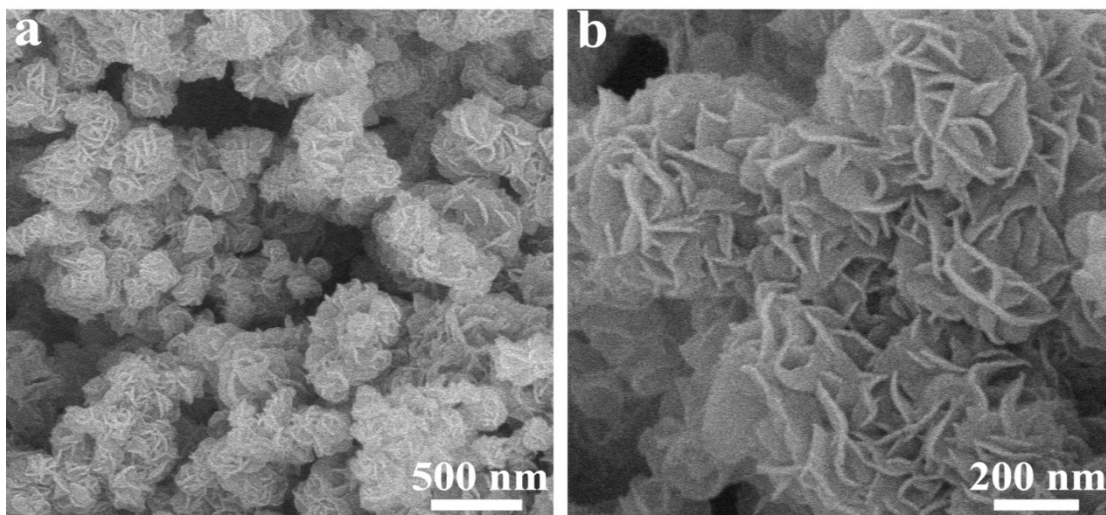
96

97 Figure S1 (a,b) SEM spectrum of MoS$_2$ nanoplates.

98

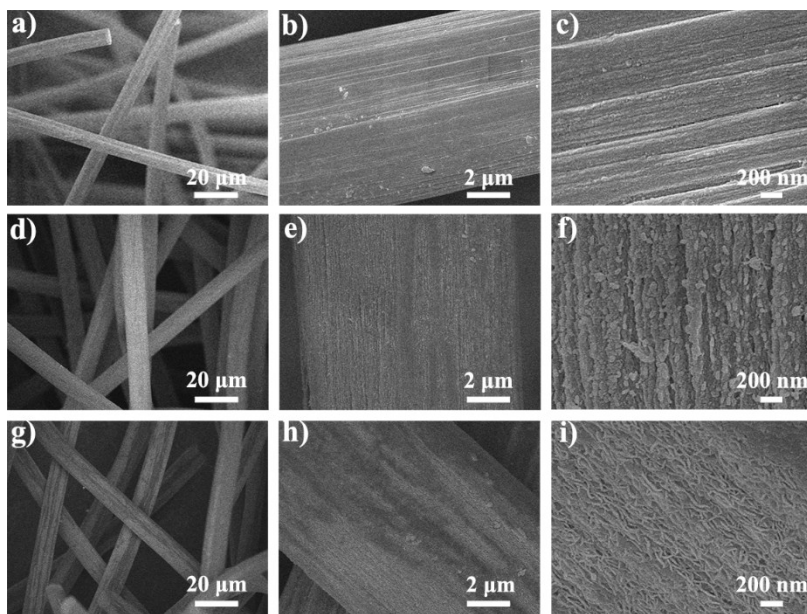99   Figure S2 Elemental analysis of MoS_2 nanoplates.

100   Table S1 EDS analysis of MoS_2 nanoplates.

Spectrum 1	Type	Concentration	wt%	wt% Sigma	% atom
S	K	17.83	43.95	2.76	70.12
Mo	L	19.85	56.05	2.76	29.88
Total			100.00		100.00

101

102

103 Figure S3. SEM images of (a−c) GF, (d−f) 15 mg MoS$_2$@GF, (g−i) 25 mg MoS$_2$@GF at

104 different magnifications.

105
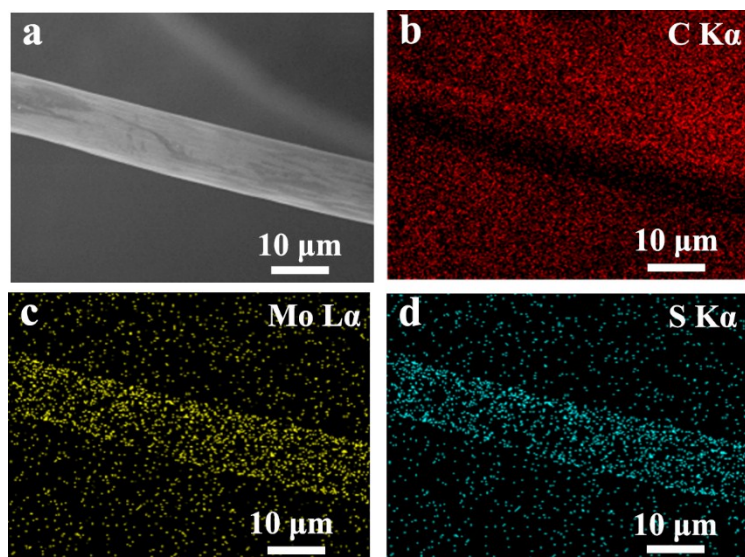
Figure S4. EDS mapping images of 20 mg MoS$_2$@GF.
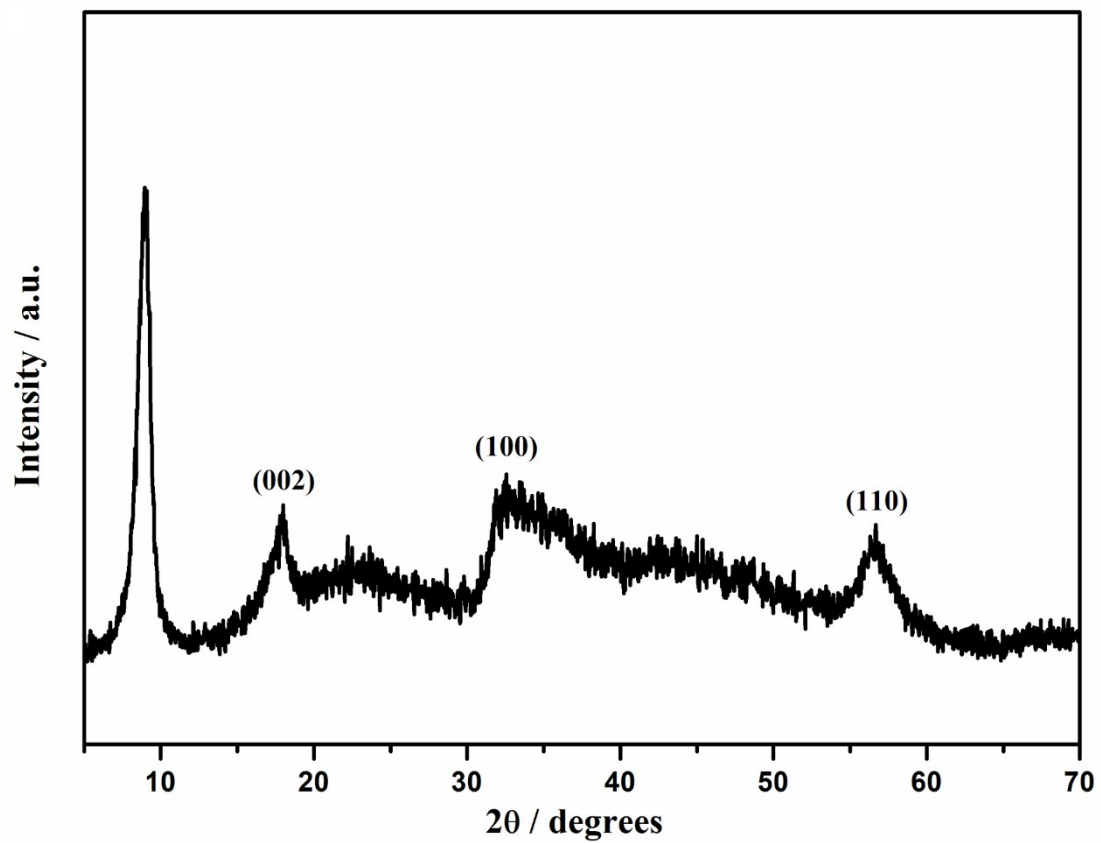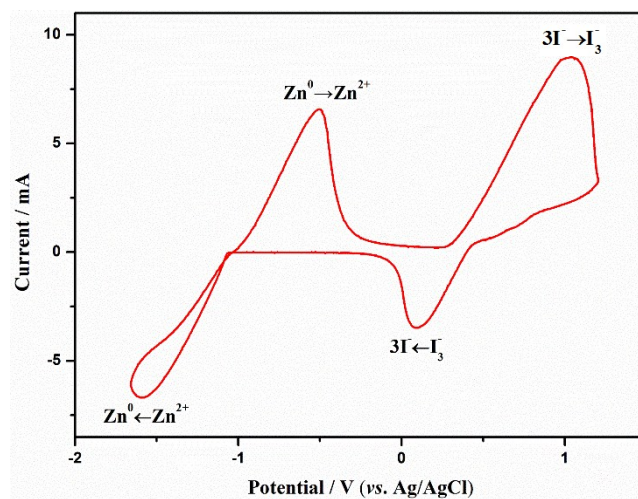
109

110 Figure S5. XRD pattern of the as−synthesized MoS$_2$.
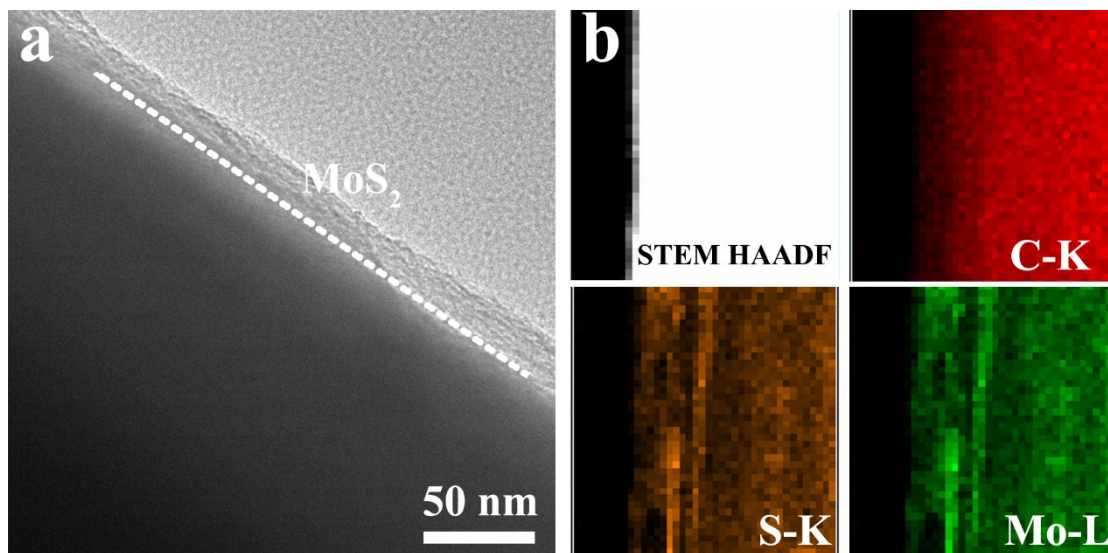
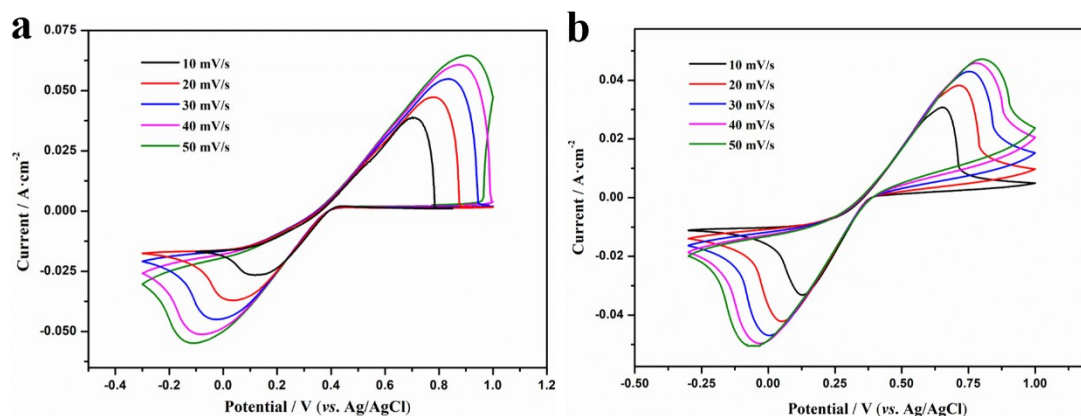Figure S6. TEM images (a) of 20mg $MoS_2@GF$ and the corresponding mapping images (b) of C, Mo, and S elements.

116

Figure S7. Cyclic voltammograms of 0.1 M ZnI_2 at the scan rate of 50 mV· s^{-1}.

Figure S8. Cyclic voltammograms of 0.1 M ZnI_2 & 0.1 M $Zn(I_3)_2$ at different scan rate on GC (a) and MoS_2@GC (b) electrode.

Table S2. Electrochemical Properties Obtained from Cyclic Voltammetry Results for GC and MoS_2@GC electrode at different Scan Rate.

| Scan rate (mV/s)	Glassy carbon		MoS_2−modified GC	
	ΔE (mV)	$\left| i_{pa}/i_{pc} \right|$	ΔE (mV)	$\left| i_{pa}/i_{pc} \right|$
10	0.582	0.685109	0.521	1.078049
20	0.740	0.778545	0.661	1.101961
30	0.860	0.820087	0.745	1.091967
40	0.955	0.841724	0.801	1.082879
50	1.015	0.848082	0.848	1.069915

127 The following equation can be utilized to calculate reaction rate constant of totally irreversible

128 reactions.

129 $$i_p = 0.227nFAC_0k^0 exp\left(-\alpha nF\frac{E_p - E_0}{RT}\right)$$

130 Where i_p is the peak current density, n is number of transfer electron during electrode reaction,

131 F is faraday constant (F = 96485 C/mol), A is surface area of the electrode (geometric area ~

132 0.2 cm^2), C_o is the electrolyte concentration (0.1 M), k^0 is the reaction rateconstant, α is the

133 symmetry coefficient and E_p is peak potential. The obtained ln i_p is proportional to $(E_p - E_o)$ with

134 a slope of $-\alpha nF/RT$ and an intercept proportional to k^0.

135
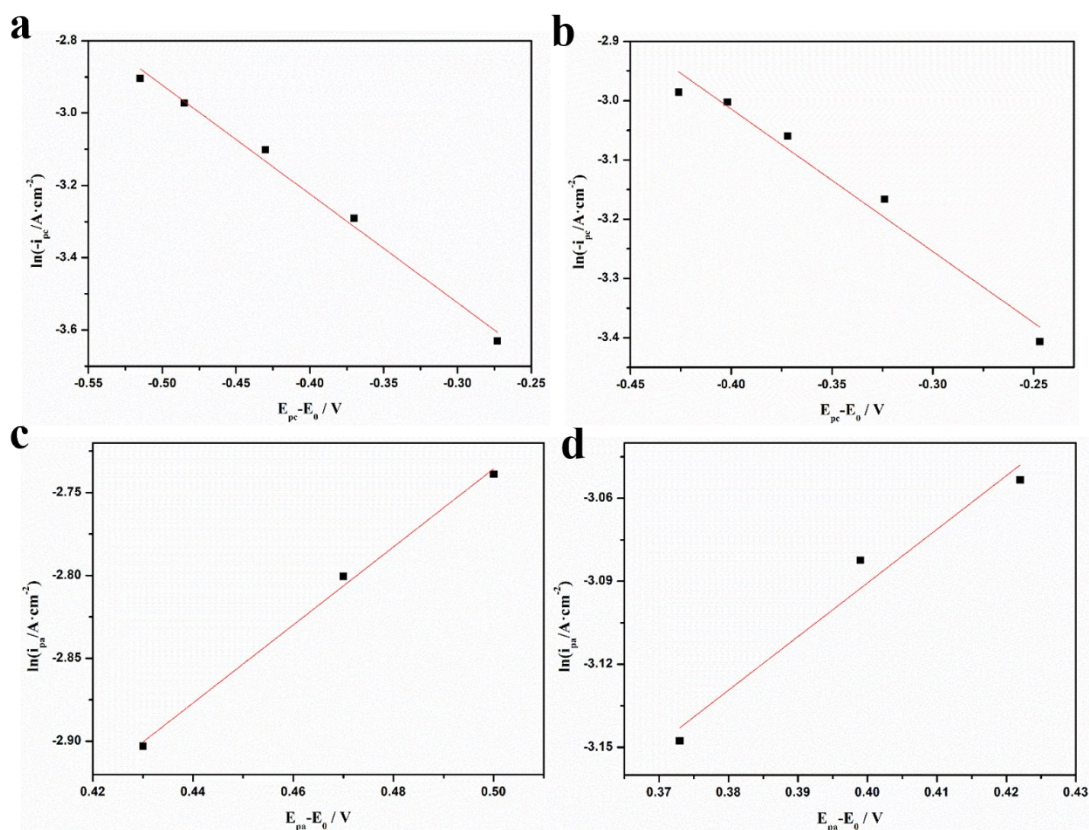
Figure S9. Plot of ln(i_p) vs. (E_p-E_0) for (a, b) reduction of triiodide ions and (c, d) oxidation of iodide ions for GC and MoS$_2$@GC electrode.

Table S3 Reaction rate constant (k^0) of GC and MoS$_2$@GC electrode for triiodide/iodide redox reactions.

Sample	Intercept (cathodic)	k_c^0 (cm·s^{-1})	Intercept (anodic)	k_a^0 (cm·s^{-1})
GC	−3.9173	0.0136	−4.4274	0.0082
MoS$_2$	−3.8659	0.0143	−3.9755	0.0128
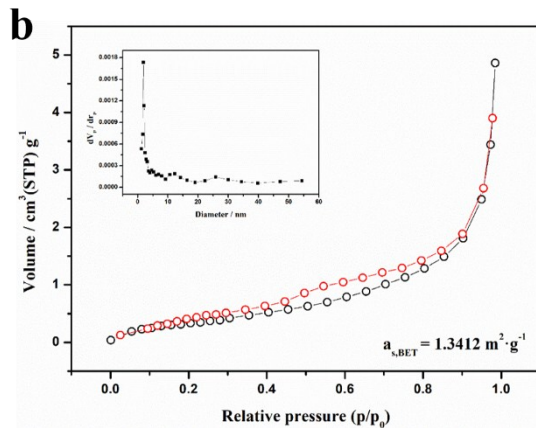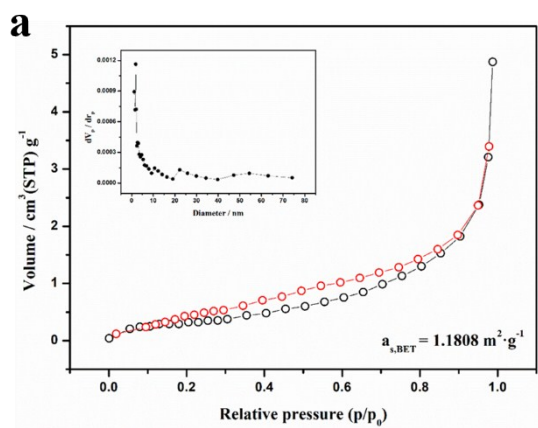
143

144 Figure S10. N_2 adsorption−desorption isotherms of GF (a) and 20 mg MoS_2@GF (b).

145

146

147　Figure S11. The structure of the non−flow cell.

148

149 The coulombic efficiency (CE), voltage efficiency (VE) and energy efficiency are determined

150 by the following equation.

$$CE = \frac{Q_d}{Q_c} = \frac{\int_0^{T_d} I_d dt}{\int_0^{T_c} I_c dt} = \frac{I_d T_d}{I_c T_c}$$

151

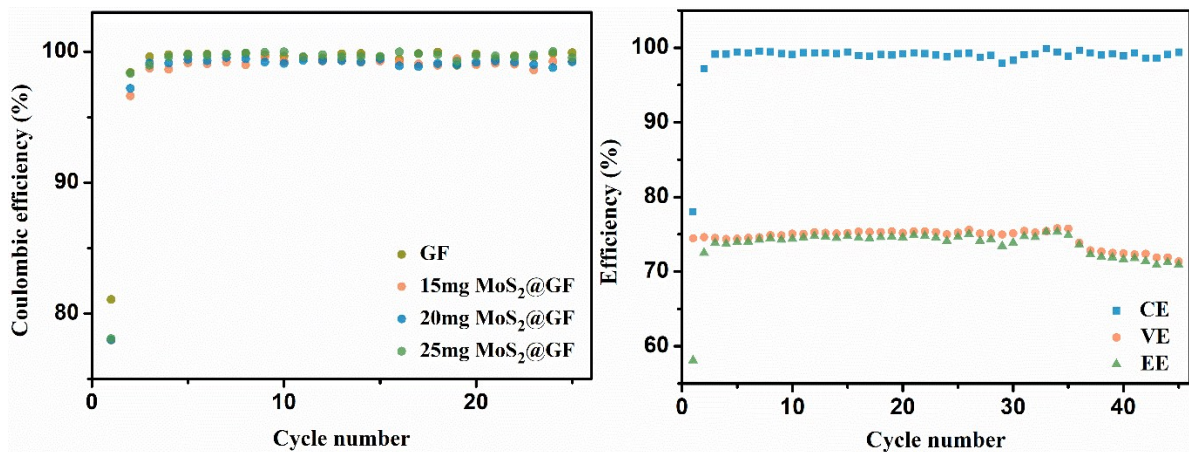$$VE = \frac{\frac{\int_0^{T_d} E_d(t)dt}{T_d}}{\frac{\int_0^{T_c} E_c(t)dt}{T_c}} = \frac{\bar{E}_d}{\bar{E}_c}$$

152

$$EE = \frac{\int_0^{T_d} I_d E_d(t)dt}{\int_0^{T_c} I_c E_c(t)dt} = \frac{I_d \int_0^{T_d} E_d(t)dt}{I_c \int_0^{T_c} E_c(t)dt} = CE \times VE$$
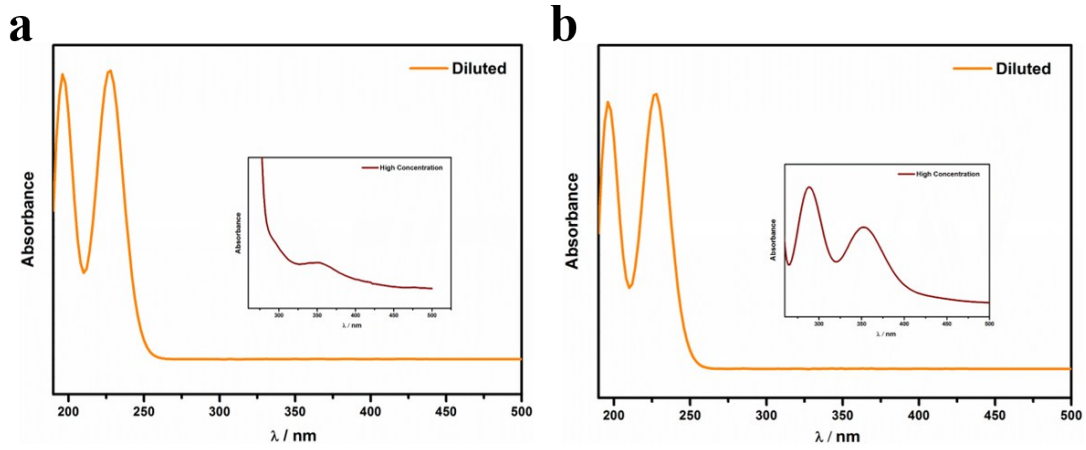
153

154 subscripts: c = charging, d = discharging, Q = charge, T= time for charging/discharging, and

155 E = potential.

156

157

158 Figure S12. (a)Coulombic efficiency with different MoS_2 loading at a current density of 30

159 mA·cm^{-2}. (b)efficiency with cycling numbers for 20 mg MoS_2@GF.

161

162 Figure S13. UV−Vis spectra of anode (a) and cathode (b) electrolyte after charge.

163 **References**

164 1 G. Kresse, D. Joubert, *Physical Review B*., 1999, **59**, 1758.

165 2 Y. Hou, D. Wang, X. Yang, W. Fang, B. Zhang, H. Wang, G. Lu, P. Hu, H. Zhao, H. Yang,

166 *Nat. Commun*., 2013, **4**, 1583.